

Journal Pre-proof

Miniaturized Forced Degradation of Therapeutic Proteins and ADCs by Agitation-Induced Aggregation using Orbital Shaking of Microplates

Florian Johann , Steffen Wöll , Matthias Winzer , Jared Snell , Bernhard Valldorf , Henning Gieseler

PII: S0022-3549(21)00497-4
DOI: <https://doi.org/10.1016/j.xphs.2021.09.027>
Reference: XPHS 2537



To appear in: *Journal of Pharmaceutical Sciences*

Received date: 1 June 2021
Revised date: 19 September 2021
Accepted date: 19 September 2021

Please cite this article as: Florian Johann , Steffen Wöll , Matthias Winzer , Jared Snell , Bernhard Valldorf , Henning Gieseler , Miniaturized Forced Degradation of Therapeutic Proteins and ADCs by Agitation-Induced Aggregation using Orbital Shaking of Microplates, *Journal of Pharmaceutical Sciences* (2021), doi: <https://doi.org/10.1016/j.xphs.2021.09.027>

This is a PDF file of an article that has undergone enhancements after acceptance, such as the addition of a cover page and metadata, and formatting for readability, but it is not yet the definitive version of record. This version will undergo additional copyediting, typesetting and review before it is published in its final form, but we are providing this version to give early visibility of the article. Please note that, during the production process, errors may be discovered which could affect the content, and all legal disclaimers that apply to the journal pertain.

© 2021 Published by Elsevier Inc. on behalf of American Pharmacists Association.

Miniaturized Forced Degradation of Therapeutic Proteins and ADCs by Agitation-Induced Aggregation using Orbital Shaking of Microplates

Florian Johann^{1,2}, Steffen Wöll², Matthias Winzer², Jared Snell³, Bernhard Valldorf², Henning Gieseler^{1,4,*}

¹Friedrich-Alexander University (FAU) Erlangen-Nürnberg, Department of Pharmaceutics, Freeze Drying Focus Group (FDG), Cauerstraße 4, 91058 Erlangen, Germany

²Merck KGaA, Department of Pharmaceutical Technologies, Frankfurter Straße 250, 64293 Darmstadt, Germany

³EMD Serono Research and Development Institute, Department of Pharmaceutical Technologies, 45A Middlesex Turnpike, Billerica, MA, 01821, USA

⁴GILYOS GmbH, Friedrich-Bergius-Ring 15, 97076 Würzburg, Germany

*To whom correspondence should be addressed: Henning Gieseler, phone: +49 931 90705678, fax: +49 931 90705679.

Email: info@gilyos.com

ABSTRACT

Microplate-based formulation screening is a powerful approach to identify stabilizing excipients for therapeutic proteins while reducing material requirements. However, this approach is sometimes not representative of studies conducted in relevant container closures. The present study aimed to identify critical parameters for a microplate-based orbital shaking method to screen biotherapeutic formulations by agitation-induced aggregation. For this purpose, an in-depth methodological study was conducted using different shakers, microplates, and plate seals. Aggregation was monitored by size exclusion chromatography, turbidity, and backgrounded membrane imaging. Both shaker quality and liquid-seal contact had substantial impacts on aggregation during shaking and resulted in non-uniform sample treatment when parameters were not suitably selected. The well volume to fill volume ratio (V_{well}/V_{fill}) was identified as a useful parameter for achieving comparable aggregation levels between different microplate formats. An optimized method (2400 rpm [a_c 95 m/s²], V_{fill} 60-100 μ L [V_{well}/V_{fill} 6-3.6], 24 h, RT, heat-sealed) allowed for uniform sample treatment independent of surface tension and good agreement with vial shaking results. This study provides valuable guidance for miniaturization of shaking stress studies in biopharmaceutical drug development, facilitating method transfer and comparability between laboratories.

KEYWORDS

forced conditions, formulation, protein aggregation, high throughput technology(s), physical stability, monoclonal antibody(s), antibody drug conjugate(s) (ADC), interfacial stress, mechanical stress

INTRODUCTION

Resulting from the labile nature of biotherapeutics, commonly encountered stresses can be detrimental to the quality of the final drug product.^{1,2} Therefore, careful development of an optimized formulation with stabilizing excipients is a crucial aspect of a stable biotherapeutic product. Novel biotherapeutics, such as fusion proteins (FPs) and antibody-drug conjugates (ADCs) are on the rise.³ These novel therapeutic modalities bring new challenges to formulation development, one of which is comparatively limited material availability in early preclinical phases. In such cases, miniaturization of formulation studies is beneficial to minimize material requirements while enabling early access to detailed stability data, which can shorten development times and provide a deeper understanding of factors impacting product stability.

A major product stability concern is protein aggregation, as it can lead to a loss of efficacy and present safety concerns related to adverse immune responses.⁴ Aggregation can be triggered by various factors such as thermal, oxidative, and interfacial stress.^{1,5} Interfacial stress occurs at air-liquid, liquid-liquid, and solid-liquid interfaces throughout the life cycle of a biopharmaceutical product from manufacturing to storage, transportation, and clinical administration.⁶ As proteins are amphiphilic molecules, they adsorb readily to the air-water interface^{7,8} where they form interfacial films.^{9,10} Agitation incurred for example by shipping,^{11,12} can result in mechanical rupture of these films and release protein aggregates into solution.^{8,13}

Various methods such as orbital shaking are commonly applied in laboratories to evaluate the susceptibility of biotherapeutics to interfacial stresses.¹⁴ These methods typically employ primary containers and fill volumes in line with the final drug dosage form.¹⁴ This approach is often associated with high material demands limiting the suitability of these methods for early formulation screening experiments. In contrast, microplates offer distinct advantages both in terms of low sample volumes and compatibility with high-throughput equipment (e.g., plate readers or liquid handlers). Microplates have been previously used in formulation studies for measuring biophysical surrogate parameters for conformational and colloidal stability, such as those obtained from thermal ramping,¹⁵⁻¹⁸ chemical unfolding,¹⁹ and self-interaction studies²⁰.

However, there is little literature available on microplate-based formulation screening by interfacial stress. Dasnoy et al.²¹ presented an air bubbling method to discriminate antigen 18A formulations by inducing continuous turn-over of air-liquid interfaces in microplates. The authors reported substantial volume loss from evaporation during air bubbling, a challenge that could be minimized by conducting shaking studies in sealed microplates. Zhao et al.²² found a stabilizing effect of polysorbate 80 formulations in a microplate shaking study focused only on IgG formulations with and without this surfactant. In contrast, Alekseychik et al.²³ performed extensive formulation screening with different buffer salts using a microplate shaking method. While their method allowed identification of stabilizing pH conditions and buffer salts for one of two IgG antibodies studied, these results were not compared to data from shaking studies conducted in vials.

The extent to which microplate shaking parameters (e.g., shaking orbit or fill volume) may impact screening results is not clear from the studies above. Different magnitudes of stress may be required to differentiate between highly stable formulations (e.g., in surfactant screenings) or

sensitive molecules (compared to IgGs). Given the discrepancies between long-term storage studies conducted in vials and microplates,^{24, 25} the comparability of formulation screening results obtained from shaking studies in these two formats is currently poorly characterized.

To fill these gaps, we systematically evaluated different orbital shakers, microplates, seals, and method parameters using an IgG₁ monoclonal antibody formulation (mAb1-His) and size exclusion chromatography (SEC). Predefined requirements for equipment suitability were (1) measurable monomer loss of mAb1-His by SEC, (2) a homogenous stress distribution over a whole 96-well plate, and (3) seal integrity. The method parameters studied include shaking frequency, concentration, time, fill volume, well size, shaking orbit, and plate material. An optimized microplate shaking method was then applied to discriminate the stabilizing effects of different formulations of two monoclonal antibodies (mAbs), a FP, and an ADC. The results were compared with those obtained from vial shaking studies conducted according to the method described by Eppler et al.²⁶ using SEC and turbidity. In addition, subvisible particles generated with both methods were counted using backgrounded membrane imaging (BMI), a relatively new particle characterization technique which uses microscopic images of particles immobilized on 96-well filter plates. This method offers a relatively high-throughput, low volume option for particle characterization while providing significantly increased sensitivity compared to classical particle characterization methods such as light obscuration.²⁷

This study outlines for the first time critical factors for a microplate-based method for screening biotherapeutic formulations by agitation-induced aggregation. The study highlights the importance of critical equipment and material evaluation and provides novel insights into the relationship between orbital shaking parameters and interfacial stress in the microplate scale. Further, it is shown that application of these novel insights provides good agreement between formulation screening results obtained following shaking in both vial and microplate formats. Finally, this paper presents parameters that facilitate comparison of shaking stress data between laboratories by accounting for the effect of different shaking devices and plate formats on the magnitude of interfacial stress applied during shaking.

MATERIALS AND METHODS

Materials

Multicompendial grade L-histidine, citric acid monohydrate, polysorbate 20 (PS20), polysorbate 80 (PS80), and Poloxamer 188 (P188) were purchased from Merck KGaA (Darmstadt, Germany). Bromophenol blue solution [0.04% (w/w)] was obtained from Alfa Aesar (Kandel, Germany). All other reagents were of analytical grade or higher and buffers were prepared with Milli-Q water (Merck KGaA, Darmstadt, Germany). Two IgG₁ monoclonal antibodies (mAb1, pI 8.5 and mAb2, pI 11.1) and a bispecific fusion protein (FP, pI 8.1) were provided by Merck KGaA (Darmstadt, Germany) in a surfactant-free formulation. To generate a model ADC, fluorescein-NHS was covalently attached to lysine residues of mAb1 as described elsewhere,²⁸ resulting in a drug-to-antibody ratio of 3.9 and a broad pI range of 5.6-8.5. Details regarding the shakers, microplates, and seals used in this study are provided in Table 1.

Sample Preparation

All proteins were formulated in 10 mM histidine pH 5.5 (His) or 10 mM citrate pH 5.5 (Cit) by tangential flow filtration using a MicroKros hollow fiber filter (PES, 20 cm², 30 kDa MWCO) connected to a KrosFlo KR2i system (Repligen, Waltham, MA). For surfactant screening, PS20, PS80, or P188 were spiked into His formulations to a final concentration of 0.01%, 0.01%, and 0.1% (w/w), respectively. Formulations were noted as follows: mAb1-His-PS20, which would be mAb1 in 10 mM histidine pH 5.5 and 0.01% (w/w) polysorbate 20. Samples were filtered using a 0.22 μm PES Millex-GP syringe filter (Merck KGaA, Darmstadt, Germany) and aliquoted under laminar flow conditions into microplates (Table 1) or Ompi SG EZ-Fill ready-to-fill borosilicate type 1 glass 2R vials (Stevanato Group, Piombino Dese, Italy). Vials were stoppered with chlorobutyl rubber stoppers with a FluroTec® coating (product facing side) and B2-40 coating (product averted side) (West Pharmaceutical Services, Exton, PA) and were crimped with an aluminum cap. Microplates were sealed with adhesive seals or heat-sealed using a PlateLoc sealer (Agilent, Santa Clara, CA) for 4 s at 180 °C.

Microplate Shaking

Microplates were shaken using high-speed orbital shakers according to the experimental designs listed in Table 2. All experiments were performed at room temperature (RT) in the dark and sample positions were randomized for each condition and replicate. The centrifugal acceleration a_c for each shaker was calculated according to equation 1 using the shaking frequency n (in s⁻¹) and shaking orbit, i.e. the orbital shaking diameter, d_o (in m)

$$a_c = (2\pi * n)^2 * \frac{d_o}{2} \quad (1)$$

The well volume to fill volume ratio V_{well}/V_{fill} was obtained by dividing the well volume V_{well} by the fill volume V_{fill} .

Vial Shaking

A vial shaking protocol was adapted from Eppler et al.²⁶ as a discriminatory benchmark method. Vials were placed horizontally in a SM-30 reciprocating shaker (Edmund Bühler, Bodelshausen, Germany) with the vial cap and bottom oriented in the direction of the linear amplitude of 3 cm. All formulations were shaken in triplicates at 200 rpm and RT for 5 days in the dark. Vials were filled with 1 mL of sample with a protein concentration of 1 mg/mL. After shaking, samples (100 μL) were transferred to PA full-area microplates (Table 1) for subsequent analyses.

Seal Integrity

Seal integrity was evaluated for each of the plate sealing methods investigated in this study by monitoring changes in liquid volume in microplate wells before and after shaking. All microplate wells were filled with 100 μL of MilliQ water and the liquid volume in each well was calculated using the geometry of a truncated cone where the liquid path length measured by near-infrared (NIR) water absorption²⁹ was used as a surrogate for liquid height. NIR absorption measurements were performed with a Spark® plate reader (Tecan, Männedorf, Switzerland). Plate seals were removed

immediately before each measurement following brief centrifugation (180 g, 30 s). Path length was calculated from the absorbance at 975 nm, corrected for the baseline at 900 nm, relative to the known water absorbance at a path length of 10 mm.

Image Acquisition of Liquid Motion

Detailed images of liquid motion in microplate wells were acquired with an EOS 80D camera (Canon, Tokyo, Japan) equipped with a 70 mm F2.8 DG MACRO lens (SIGMA, Rödermark, Germany). High-speed images of the lateral well walls were collected from a distance of ~20 cm using an aperture of F5.6 and exposure time of 1/8000 s. Sufficient illumination for subsequent image analysis was achieved using a KL 1500 LCD light source (Schott, Mainz, Germany). Samples were stained with 0.002% bromophenol blue for better contrast to the transparent well walls. Images were analyzed using Fiji software (V1.51), where a pixel ratio of the maximum observed liquid height to the total well height was derived from each image. From this ratio and the known well heights listed in Table 1, the maximum liquid height for each well was calculated. The reported average maximum height (\pm SEM) was obtained from six images acquired from two separate wells (three images per well).

Size-Exclusion Chromatography

A TSKgel Super SW3000 (4.6 mm x 300 mm, 4 μ m) column (Tosoh Bioscience, Griesheim, Germany) and Agilent 1100 module (Agilent, Santa Clara, CA) with UV detection at 214 nm were used to separate high molecular weight species (HMWS), monomer, and fragments by size. The mobile phase was 0.05 M sodium phosphate (pH 6.3) with 0.4 M sodium perchlorate. The flow rate was 0.35 mL/min and the total injected protein mass was 10 μ g. Samples were diluted only for concentrations greater than 10 mg/mL in placebo buffer. Microplates were centrifuged (180 g, 15 min) and the supernatant was injected so that all HMWS were referred to as soluble aggregates. Monomer recovery was calculated from the area of the monomer peak after shaking divided by the area of the monomer peak before shaking. Reduced monomer recoveries can reflect various causes, such as the formation of insoluble and soluble aggregates. Soluble aggregates were calculated by the relative HMWS peak area to total peak area. Relative monomer loss rates were calculated from the difference between the initial monomer recovery (100%) and the monomer recovery after shaking for 24 hours. Absolute monomer loss rates were then calculated from the product of the initial concentration and the relative monomer loss rate.

Turbidity by UV-Vis Spectroscopy

Turbidity was defined as photometric optical density at 350 nm or 650 nm using a Spark[®] plate reader (Tecan, Männedorf, Switzerland). Wavelengths were selected at which neither the known intrinsic protein chromophores nor the model ADC payloads absorbed so that increases in optical density could be attributed to light scattering by insoluble aggregates. Before each measurement, microplates were centrifuged (180 g, 10 s) to remove liquid droplets from the seal. The original seal was then removed and replaced with a new UV-transparent seal (PN 6575, Corning, NY). Forty-nine independent readings were averaged for each absorbance measurement to minimize any artifacts resulting from inhomogeneous particle distributions. Measurements were distributed in a 7 x 7 circular array in the wells while a minimum distance of 1.5 mm from the well walls was maintained.

Backgrounded Membrane Imaging (BMI)

Subvisible particles larger than 2 μm were quantified by BMI using a HORIZON[®] system (Halo Labs, Burlingame, CA). Under laminar flow conditions, 30 μL of each sample was pipetted onto a 96-well polycarbonate filter plate (Halo Labs) and subsequently drawn through the filter plate under vacuum (450 mbar). This procedure removed all the liquid from the plate while particles greater than 0.4 μm were retained on the membrane surface. The membrane surface for each well was imaged before and after this procedure so that the membrane background could be subtracted from the sample image. This method ensured that only particles originating from the sample were counted and sized during image processing with the HORIZON VUE software (V1.3.4). Where necessary, samples were diluted in their respective buffers prior to filtering to ensure the membrane coverage remained below 4%.

Surface Tension

Surface tension was measured by drop shape analysis with a DSA25 (Krüss, Hamburg, Germany). Using a 15G needle and syringe, droplets were formed within a closed glass cuvette to minimize the effect of evaporation and air convection on drop shape analysis. Images were acquired at a rate of 1 frame per second for 60 minutes. The surface tension was calculated from the drop shape using Krüss Advance software (V1.11) based on the Young-Laplace equation. Surface tension after 30 min was averaged using 20 data points.

Viscosity

Viscosity was measured using a HAAKE RheoStress 1 rheometer equipped with a C60/0.5° Ti or C35/0.5° Ti L cone (Thermo Fisher, Waltham, MA). All samples were equilibrated to 20 °C using a Peltier plate before each measurement. During each viscosity measurement, the shear rate was ramped twice per sample from 0.1 to 10000 s^{-1} . Shear rate versus shear stress profiles were fitted by linear regression. Since viscosity in this range was independent of shear rate for all samples, viscosity was extracted using the slope of the linear fit according to Newton's law of viscosity.

Statistical Data Analysis

Data are presented as mean (\pm standard deviation), unless otherwise stated. Differences are given with the 95% confidence interval (CI). Statistical calculations were carried out using GraphPad Prism V9.0.0. Multiple comparisons were performed by two-way ANOVA following Bonferroni's method (post hoc test). Data from $V_{\text{well}}/V_{\text{fill}}$ curves were fitted and compared by the Simple Linear Regression module in Prism, which compares slopes and intercepts. Significance is indicated by * $p < 0.05$, ** $p < 0.01$, *** $p < 0.001$.

RESULTS AND DISCUSSION

Impact of Shaker on Well Position Effects

The first step in the development of a microplate-based shaking stress method was identifying suitable shakers that induced measurable mAb1-His monomer loss and allowed comparison between samples independent of their well position. Three high-speed orbital microplate shakers (further denoted as Shaker A, Shaker B and Shaker C) were characterized by measuring monomer recoveries of mAb1-His for all wells in 96-well plates after shaking (Figure 1). Notably, Shaker A and C had shaking orbits of 3 mm while Shaker B differed with an orbit of 2 mm. Differences in shaking orbits would result in different centrifugal accelerations a_c for a given shaking frequency. Under the hypothesis that a comparable stress input is obtained using a similar a_c , the shaking frequency for each shaker was adjusted to achieve an a_c of $\sim 100 \text{ m/s}^2$. This corresponded to the maximum feasible speed of Shaker B (3000 rpm) and to 2500 rpm for Shaker A and C. Using these conditions, after 24 hours of shaking similar monomer recoveries of $\sim 80\%$ were obtained in the center of the microplates for all shakers.

Unexpectedly, monomer recoveries gradually decreased toward the plate edges for Shaker A (to $\sim 55\%$) and to a lesser extent for Shaker B (to $\sim 65\%$). In contrast, Shaker C exhibited homogeneous monomer recovery across all wells. Over an entire plate the coefficient of variation (CoV) for monomer recovery was 10.3%, 8.0%, and 4.2% for Shaker A, B, and C, respectively. Further, the maximum differences between microplate column means were 16.6% [CI 10.2-23.0%], 10.4% [CI 2.4-20.4%], and 5.1% [CI 0.7-9.5%] for plates shaken with Shaker A, B, and C, respectively. Hence, Shaker C was selected for most subsequent studies and sample positions were randomized to further minimize residual well position effects.

Impact of Shaking Frequency on Well Position Effects

We hypothesized that well position effects might be greater near the maximum shaking frequency for each shaker. To test this assumption, shaking parameters were adjusted for Shaker A, which showed the greatest well position effects. To investigate a possible device-dependent effect of shaking frequency on well positions effects, shaking frequency was increased while maintaining comparable levels of monomer recovery. Monomer recoveries after shaking were maintained by reducing the shaking time from 24 to 5 hours while simultaneously increasing the shaking frequency from 2500 rpm to 3000 rpm. Increasing the shaking frequency to 3000 rpm resulted in a significant increase in well position effects with a maximum difference in column means of 25.2% [CI 20.4-30.0%] and plate CoV of 22.8%. Consequently, a device-dependent effect of shaking frequency on well position effects must be suspected for Shaker A.

At high shaking frequencies (2500-3000 rpm) Shaker A visually exhibited irregular orbital motion, in which the shaking platform moved not only in a horizontal circular motion but also in a slight upwards and downwards wobbling motion. This movement likely resulted from the shaking platform being connected to the device by a single central axis that could not stabilize the platform at higher frequencies. This irregular orbital motion could induce incrementally greater mechanical stress as the distance of the wells to the central axis increased and correlated with the observed well position effects.

An additional consideration is that heat dissipated during extended and / or high-speed shaking could contribute to positional effects. We evaluated possible heat dissipation for all three shakers included in the current study by measuring sample temperatures for six randomly selected wells after shaking for 24 hours at 2500 rpm. Negligible increases in temperature were found for all

shakers (< 3.6 °C) with no dependence on well position. We would like to highlight that heat dissipation could vary between different models and manufacturers of shakers and should be considered when selecting shaking frequency and duration.

Seal Integrity

Well position effects have also been reported in terms of evaporation in microplate-based storage studies, ranging from 7% to 20% volume loss from the plate center to the plate edges after 30 days of storage at 37 °C.²⁴ Evaporation was correlated with a position-dependent increase in aggregates.²⁵ In comparison, the short time frame (1 day) and low temperature (23 °C) used in the present study presents a low risk for evaporation. However, high centrifugal forces during high-speed shaking may compromise seal integrity causing volume loss by liquid spillover.

We evaluated seal integrity of the two seals selected for this study by measuring volume losses for all 96 wells of sealed and shaken microplates. Microplates sealed using adhesive seals exhibited up to 23% volume loss in only a few wells in the outer perimeter, while heat-sealed plates showed excellent volume recovery in all wells (>96%). Far higher volume losses of 30% were reported when interfacial stress was induced with an air bubbling method.²¹ While heat-sealed plates provided superior volume recovery, the heat-sealing process involves briefly exposing the surface of the plate to temperatures of 180 °C. We found that this brief exposure resulted in temperature excursions less than 5 °C for samples in each well and no monomer loss could be detected for mAb1-His by SEC following heat sealing.

Heat sealing was selected as the preferred sealing method for subsequent studies, because, in addition to superior seal integrity, it can be readily automated and reduces operator biases associated with plate sealing (e.g., inconsistent pressure when applying adhesive seals). Overall, our observations suggest that volume loss appears to be a minor problem in microplate-based shaking studies.

Impact of Formulation on Liquid Motion During Shaking

After verifying that shaking stress could be homogeneously applied in a 96-well plate format and that volume loss could be minimized, we shifted our focus to parameters impacting the magnitude of interfacial stress applied during shaking. We evaluated the behavior of liquid formulations of mAb1-His within the wells of a microplate as a function of shaking frequency (Figure 2). Images acquired during shaking showed that liquid motion can be divided into three stages as the shaking frequency increases. First, no liquid motion was observed macroscopically for shaking frequencies between 0 and 500 rpm (I). Then, above a minimum shaking frequency n_{min} , the liquid height increased steadily (II) and was finally limited by the seal (h_{max}) above a shaking frequency n_{max} (III). For mAb1-His with a 100 μ L fill volume, n_{min} was between 500 and 700 rpm and n_{max} was between 1500 and 1700 rpm.

In this study the liquid height was used as a surrogate metric for tracking the effect of different formulation compositions on the air-liquid surface area. As illustrated in Figure 3A, at moderate shaking frequencies between n_{min} and n_{max} , the liquid height in each well was dependent on the formulation composition. The parameter n_{min} is strongly dependent on the surface tension of the

sample, and thus defined by the point when centrifugal forces overcome surface tension.³⁰ The equilibrium surface tensions as measured after 30 min were 73.4 (± 0.9), 57.6 (± 0.1), and 38.3 (± 0.6) mN/m for Placebo-His buffer, mAb1-His, and mAb1-His-PS20, respectively. Accordingly, the lower the surface tension, the earlier we observed an increase in liquid height, with n_{min} and n_{max} of mAb1-His-PS20 < mAb1-His < Placebo-His. In contrast, the viscosity was similar for Placebo-His, mAb1-His, and mAb1-His-PS20 with water like values of ~ 1 mPas at a protein concentration of 1 mg/mL. Therefore, it can be postulated that the surface tension of each formulation directly impacts the air-liquid surface area in the range between n_{min} and n_{max} (II).

Impact of Shaking Frequency on Monomer Recovery

Trends in monomer recovery as a function of shaking frequency are shown in Figure 3B and can be compared directly with liquid height plotted in Figure 3A. As the air-liquid surface area increased above n_{min} , a significant reduction in monomer recovery of mAb1-His was observed. However, monomer recoveries remained high ($\sim 97\%$ at 1350 rpm) when the shaking frequency was maintained between n_{min} and n_{max} . Computational fluid dynamics simulations have shown that compared to shaking with a vortex mixer, orbital shaking induces relatively small increases in air-liquid surface area.³¹ This may explain high monomer recoveries at moderate shaking frequencies.

At shaking frequencies above n_{max} (III), monomer recoveries began to decrease substantially. It is important to note that at these higher frequencies monomer recovery continued to decrease, although further enlargement of the air-liquid interface appears to be somewhat limited. Interestingly, at these high shaking frequencies, monomer recoveries differed significantly between plates sealed with the adhesive and heat seal. Possible reasons for this behavior will be discussed below.

Degradation Behavior upon Seal Contact (above n_{max})

We have considered multiple potential explanations for the impact of the seals and the continued decrease in monomer recovery for shaking frequencies above n_{max} . First, as leachable or extractable compounds from plastics have been identified as potential sources of interference in bioassays and immunological studies,^{32,33} we selected materials to minimize potential sources of contaminants in our studies. We chose the heat and adhesive seal (Table 1) due to an absence of unknown peaks that were detectable for other seals in reversed-phase chromatography with evaporative light scattering detection (data not shown).

It is well known that monoclonal antibodies adsorb or adhere readily to solid surfaces.^{34,35} The reduction in monomer recovery presented in Figure 3B could result from the formation of insoluble aggregates or adsorption to the plate seals, as soluble aggregates detected by SEC were negligible. However, the samples shaken with the adhesive seals exhibited increased turbidity (210 mAU [CI 160-250 mAU] at 2100 rpm after 24 h) relative to those shaken with heat seals. This difference in insoluble aggregate generation between the two seal types suggests the adhesive seal may promote protein aggregation and particle formation during shaking. To further challenge the adsorption hypothesis, we incubated microplates containing mAb1-His for 24 hours in an upside-down orientation to maximize contact with the seals. Following quiescent incubation, no monomer loss was detected by SEC for mAb1-His solutions in contact with either seal type.

Adsorption of protein to the seals, though not measurable by SEC, could still promote aggregation. A synergistic mechanism of protein adsorption to siliconized syringe walls and release of aggregates by the air-liquid interface was proposed in an agitation study of siliconized syringes containing an air bubble.³⁶ Likewise, exchange may occur between the bulk solution and the seal surface as shear forces disrupt adsorbed layers. Differences in adsorption rates to the adhesive seals or the dynamics of intermolecular rearrangements, aggregation and gel formation upon adsorption may result in greater insoluble aggregate formation compared to the heat seals. Such solid-liquid interfacial stress is discussed further in the sections on fill volume and plate materials.

Further explanations for the continued decrease in monomer recovery above n_{max} could be mixing and compression / dilation^{13,37} related effects. Faster mixing at higher shaking frequencies could promote aggregation by rapidly exchanging monomers and aggregates between the liquid bulk and the air-liquid interface. Further, a substantial increase in particles was reported in an orbital vial shaking study as the liquid reached the top of the vial.³⁸ The authors of this study attributed this increase to compression / dilation of the air-liquid interface upon contact with the top surface of the vial at elevated speed. Similarly, in microplates the air-liquid interface may experience compression / dilation upon seal contact. In addition, differences in seal geometries may result in varying degrees of dilation (planar geometry for adhesive and dome-like geometry for heat seals), explaining the impact of seals for shaking frequencies greater than n_{max} . Overall, the results suggest that seal properties could impact data obtained from shaking stress studies and should be considered when comparing results between laboratories.

Rationale for Shaking Frequency Selection

For further studies described in this work a shaking frequency of 2400 rpm (a_c 95 m/s²) was selected. The shaking frequency was adopted because a high shaking frequency enables (1) a limited, hence similar, air-liquid surface area and (2) liquid-seal contact for all samples despite differences in surface tension. This frequency ensured liquid-seal contact for all conditions studied, including those with low fill volumes and high concentration (i.e., 100 mg/mL) formulations (data not shown). (3) Increased stress input at high frequencies may provide improved discrimination between formulation conditions. This shaking frequency provided (4) a safety margin to the shaker's operating maximum to avoid amplification of well position effects as observed for Shaker A. We experienced (5) issues with equipment durability when shaking at higher frequencies for multiple days.

Impact of Initial Concentration and Time

The effect of the initial mAb1-His concentration c_0 on monomer loss rates during shaking was examined over a concentration range from 0.2 to 100 mg/mL (Figure 4A). The slope of the dashed line in Figure 4A indicates a first-order scaling of the absolute monomer loss rates with protein concentration. At low concentrations (0.2 to 10 mg/mL), there was a weak relationship between initial concentration and absolute monomer loss rates (below first-order dependency). Therefore, relative monomer loss rates appear to decrease with increasing c_0 . Consistent with this, linear kinetics (zero-order) were obtained over a 96 hour shaking period with a c_0 of 1 mg/mL (Figure 4B). The weak dependence of absolute monomer loss rates on protein concentration in the lower concentration range is in excellent agreement with prior observations from compression / dilation experiments^{13,39} and vial shaking⁴⁰. The resulting inverse relationship between relative aggregation

rates and protein concentration was attributed to the air-liquid interfacial area being the rate-limiting factor for agitation-induced aggregation.⁴⁰

Samples at concentrations greater than 12.5 mg/mL exhibited increased viscosities (η), which affected liquid motion (data not shown). For mAb1-His at 100 mg/mL (η 23.1 mPas, V_{fill} 100 μ L), n_{max} increased to 2100-2300 rpm. The implications of such a shift in n_{max} were previously discussed in the sections on liquid motion and shaking frequency (selection). We want to emphasize that this shift in n_{max} may also be relevant for samples formulated with excipients that yield solutions of high viscosities.

At concentrations greater than 25 mg/mL absolute monomer loss rates approached first-order dependence on concentration. Further studies are required to elucidate how properties of high concentration formulations such as viscosity impact agitation-induced aggregation rates. For further studies described here, a sample concentration of 1 mg/mL was selected to reduce material consumption and to achieve both high (relative) monomer loss in SEC and linear kinetics. The latter may allow for comprehensive stress scalability based on shaking time.

Impact of Fill Volume

An inverse relationship between the fill volume V_{fill} and mAb1-His monomer loss after microplate shaking was observed (Figure 5A). After 24 hours of shaking, complete mAb1-His monomer recovery (\sim 100%) was observed for entirely filled wells (360 μ L), reducing the fill volume to 60 μ L decreased monomer recoveries to 72.9% (\pm 2.6) and 32.4% (\pm 3.2) for plates sealed with heat and adhesive seals, respectively. A fill volume of 100 μ L was selected for a general method as this fill volume provided both an adequately high stress input and sufficient volume for subsequent analytics.

Kiese et al.⁴¹ reported that eliminating headspace by completely filling vials resulted in negligible aggregation during shaking, while aggregation was observed when headspace was present in partially filled vials. The authors concluded that aggregation during shaking was due to air-liquid rather than glass-liquid interfacial stress. In alignment, no monomer loss was detected in fully filled microplate wells in the present study. This suggests that the monomer loss induced by shaking partially filled microplate wells may likewise be attributed to air-liquid rather than to solid-liquid interfacial stress. The latter was previously proposed to explain the differences in monomer recovery upon liquid-seal contact when using different seals. Based on the findings in this section, the impact of seals is unlikely to be explained by solid-liquid interfacial stress alone. Likewise, adsorptive loss resulting from monomer adsorption to the seals seems unlikely since the samples without headspace were in direct contact with the entire seal surface during shaking. However, a synergistic effect of the air-liquid and seal-liquid interfaces on aggregation cannot be excluded.

Impact of Well Size

The relationship between fill volume and monomer recovery was non-linear, independent of seal type (Figure 5A, top panel). In contrast, normalizing the fill volume V_{fill} by the total well volume V_{well} , resulted in a linear correlation between the V_{well}/V_{fill} ratio and monomer recovery with a

regression coefficient (R^2) of 0.96 and 0.97 for the heat and adhesive seal, respectively (Figure 5A, bottom panel).

On this basis, we investigated whether the V_{well}/V_{fill} ratio could be applied to achieve comparable stress levels when samples were shaken in full-area (V_{well} 360 μ L) and half-area (V_{well} 210 μ L) plates. First, a shaking orbit must be selected that is appropriate for the respective plate. The orbital shaking diameter d_o should be smaller than the well diameter to facilitate mixing instead of centrifugation, but not so small that the probability for unfavorable “out-of-phase” conditions increases.⁴² Both microplate formats were tested on Shaker B, which is compatible with a wide range of microplate well diameters even up to the 384-well format due to its 2 mm shaking orbit.

Samples shaken in half-area plates exhibited higher monomer recoveries than those in full-area plates with similar fill volumes after shaking for 24 hours (Figure 5B, top panel). After normalizing the results using the V_{well}/V_{fill} ratio, the curves were indistinguishable both by slope ($p=0.91$) and intercept ($p=0.51$) (Figure 5B, bottom panel). This suggests comparable stress levels are applied when the fill volume is adjusted to achieve similar V_{well}/V_{fill} ratios in half-area and full-area plates.

For further clarification, the common terminologies “full-area” and “half-area” for microplates refer to the circle base area of the well bottom. However, stress levels were *not* comparable when normalized using the area A of the well bottom (significantly different A/V_{fill} curve intercepts, $p<0.01$). Except for high fill volumes, the liquid rotates mainly along the well walls above n_{max} (Figure 2). Therefore, the well bottom area may be less relevant for the stress applied during shaking.

Nevertheless, these results may be limited to the well geometry of a truncated cone. We previously discussed compression / dilation of the air-liquid interface as a mechanistic explanation for the observed monomer loss behavior upon liquid-seal contact. Such compression / dilation could also be relevant in non-cylindrical well geometries, such as for edges for plates with square well geometry.

Impact of Shaking Orbit

Due to the necessity of a smaller shaking orbit d_o for smaller well sizes, we investigated how comparable stress levels can be achieved when using shakers with different d_o . As indicated in the studies on well position effects, centrifugal acceleration a_c could be suitable for this purpose, but a direct comparison was difficult due to well position effects observed at 3000 rpm for Shaker B. However, well position effects were sufficiently low (CoV 6.7%) when Shaker B was operated at shaking frequencies below 2500 rpm, allowing the direct comparison of Shaker C (d_o 3 mm) and Shaker B (d_o 2 mm).

A shaking frequency of 2400 rpm resulted in similar monomer recoveries for 2 mm (a_c 63 m/s^2) compared to 3 mm (a_c 95 m/s^2) shaking orbits (Figure 5C). Using a similar centrifugal acceleration of 66 m/s^2 , corresponding to 2000 rpm for the 3 mm shaking orbit, resulted in higher monomer recoveries in comparison. However, the V_{well}/V_{fill} curves were different in slope ($p<0.05$) at both conditions. These trends indicate better comparability between results when the shaking frequency is maintained for shakers with different shaking orbits. Nevertheless, there may be instances where the shaking frequency should be increased when using smaller orbits, for example, when higher centrifugal forces are required to ensure liquid-seal contact for all samples.

Impact of Plate Material

Three plate materials, namely polypropylene (PP), polystyrene (PS) and polyacrylate (PA) were compared by measuring mAb1-His monomer recovery after shaking. Since heat sealing induced a small shrinkage in well height for polypropylene plates of 0.6 mm, adhesive seals were selected for this study to ensure similar well dimensions for all plate materials. For the plate materials studied no significant difference in mAb1-His monomer recovery was detected. This result suggests that either stress incurred at the air-liquid interface is the dominant source of aggregation during shaking or that the three plate materials resulted in little difference in the stress incurred at the solid-liquid interface. All other shaking studies described in the present study were conducted with PA microplates. This selection was based solely on their UV-Vis-transparent bottoms, which enabled direct use with analytical methods such as turbidity.

Comparability of Formulation Screening Results After Shaking in Vials or Microplates

Based on the findings described above for mAb1-His, an optimized microplate shaking method was developed (2400 rpm [a_c 95 m/s²], V_{fill} 100 μ L [V_{well}/V_{fill} 3.6], 24 h, RT, heat-sealed PA full-area plates, Shaker C). Using this shaking method, good intra-plate (CoV 0.9%) and inter-plate (CoV 1.5%) reproducibility for mAb1-His monomer recovery after shaking was demonstrated (Table 3). RT was selected for this method as moderate temperatures accelerate surface-mediated aggregation rates, while the increase in bulk-mediated aggregation rates may be negligible.³⁹ In the present study, non-shaken (quiescent) controls incubated at RT for five days showed no significant monomer losses. Thus, reduced monomer recoveries may be attributed to surface-mediated rather than bulk-mediated aggregation during shaking. The comparability of this optimized microplate method to vial shaking was evaluated by comparing four different biotherapeutic modalities formulated using different buffer salts (His and Cit) and surfactants (PS20, PS80, and P188).

Monomer recoveries measured after shaking exhibited similar trends across the two shaking formats studied (Figure 6). Focusing on the two buffer systems (histidine and citrate) without added surfactants, a clear stabilizing effect of histidine buffer for both mAb1 and ADC was identified with both shaking formats. However, only after shaking in a microplate format was a statistically significant increase in monomer recovery for mAb2 in histidine buffer relative to citrate observed. Vial shaking also showed a possible stabilizing effect for mAb2 in histidine buffer but resulting from a comparatively high CoV (10.3%) the results were not considered statistically significant. Finally, the extent of monomer loss for FP in both buffers was so extensive (<1.6% monomer recovery) following shaking in either format that the two formulation conditions could not be differentiated. For both formulation conditions, soluble aggregates detected by SEC were negligible, suggesting that reductions in monomer recovery could be attributed to the formation of insoluble aggregates. This conclusion was confirmed by turbidity and particle measurements (Figure 7).

An important application of a microplate-based shaking method would be to elucidate the effects of structural modifications on the susceptibility of molecules to interfacial stresses. For this purpose, the ADC selected for this study was a lysine-fluorescein conjugate of mAb1. This provided an opportunity to investigate the effect of conjugation on mAb1 interfacial stability. Gandhi et al. previously reported increased agitation-induced aggregation for lysine-conjugated trastuzumab emtansine compared to the unconjugated mAb.⁴³ Using both shaking formats our study showed a

similar destabilization of conjugated mAb1 resulting in reduced monomer recovery following shaking (Figure 6). More importantly, this result demonstrated that a microplate shaking protocol could be applied to applications beyond formulation screening.

Surfactants are well known to be excellent stabilizers against agitation-induced stress.^{8, 41, 44} The stabilizing effect of surfactants was apparent for all biotherapeutics modalities investigated in the current study regardless of shaking format. For samples containing surfactant, only the ADC exhibited reduced monomer recoveries with 65.4% (± 2.4) (PS20), 94.5% (± 0.1) (PS80), and 98.5% (± 0.2) (P188) monomer remaining after shaking in vials (Figure 6A). For ADC formulations containing PS20 and PS80, soluble aggregate content increased from 2.9% (± 0.1) before shaking to 10.5% (± 2.8) (PS20) and 4.6% (± 0.2) (PS80) after shaking in vials. However, the mass of soluble aggregates in these samples did not account for the total mass of monomer lost during shaking, suggesting that agitation-induced stress promoted the generation of insoluble aggregates. This was supported by increases in turbidity and particle concentrations for these conditions (Figure 7). In contrast, no monomer loss was observed after microplate shaking based on SEC results. The high stability of mAb1, mAb2, and FP in surfactant-containing formulations may be attributed to the comparatively high surfactant concentrations studied, since in other studies lower surfactant concentrations (e.g., 0.0025%⁴¹ or 0.0005%⁴⁴ PS20) were sufficient to inhibit aggregation.

Resulting from the limited sensitivity of SEC, all aggregates generated during shaking may not be detected by this analytical method. Increases in subvisible particle concentrations, while an early indicator of protein aggregation, may account for a minuscule percentage of the total protein in solution. Prior shaking studies conducted in vials have reported increases in subvisible particle concentrations far before changes were detected by less sensitive analytical methods such as SEC or turbidity.⁴¹ Likewise, quantification of subvisible particle concentrations by BMI in the current study further differentiated the effects of the three surfactants on the stability of the ADC molecule shaken in a microplate format. For the ADC molecule, formulating with PS20 resulted in a significant increase in subvisible particles ($\geq 2 \mu\text{m}$) compared to samples formulated with either PS80 or P188 (Figure 7B). This trend was also evident for larger particles ($\geq 10 \mu\text{m}$) (Figure 7C). Further characterization of the shaken ADC formulations resulted in agreement between the two shaking formats indicating that PS20 stabilized the ADC during shaking less effectively than PS80 or P188.

The results presented above illustrated that our plate-based shaking protocol could be applied to rank formulations according to their stabilizing effect against agitation-induced stress. These rankings were generally aligned with those obtained using a standard vial shaking protocol. However, the differences between the stabilizing effects of the three surfactants for the ADC were not as clearly delineated using our microplate-based shaking protocol. This difference can likely be attributed to the magnitude of interfacial stress applied by both shaking methods. Significantly greater monomer losses and subvisible particle concentrations (~ 2 orders of magnitude) were measured for ADC surfactant formulations shaken in vials, suggesting this protocol induced more interfacial stress. The magnitude of interfacial stress applied in both shaking formats does not need to be equivalent, however the applied stress must be sufficient to differentiate between formulation conditions while not inducing complete degradation. Improved differentiation of ADC formulations containing surfactants may be achieved by increasing the shaking stress applied in the plate format. A strategy to tailor the applied stress for screening a wide range of formulation conditions in microplates is described below.

Tailoring Stress Input by Adjusting V_{well}/V_{fill}

It is widely recognized that all biological molecules do not exhibit the same interfacial stability.^{7, 45} Therefore, any method designed to differentiate between the stabilizing effects of different formulations must be tailored depending on the molecule and formulation components studied. This was exemplified by our attempt to differentiate between the stabilizing effects of histidine and citrate buffer (without surfactant) for all four biological modalities using a single shaking protocol. While the shaking protocol performed well for the two mAbs and the ADC, the FP was completely degraded after 24 hours. Clearly, the stress applied in this protocol was too high for this specific molecule and a tailored method would be required if differentiation between the two surfactant-free conditions was desired for FP.

Generally, our results suggested that the stress applied during shaking may be scalable by time or V_{well}/V_{fill} ratio. Increasing stress by lengthening the shaking time results not only in a longer run time but also in the requirement to check at multiple timepoints whether a discriminative stress level was reached. Variation of the V_{well}/V_{fill} ratio provides the ability to scale stress within a single experiment while maintaining a single endpoint.

Decreasing the V_{well}/V_{fill} ratio from 3.6 to 2 by increasing the fill volume from 100 μL to 180 μL will reduce the total stress applied over a 24 h shaking experiment. As shown in Figure 6B, increasing the fill volume resulted in a significant increase in FP monomer recovery for samples formulated in histidine or citrate buffer without surfactant. Further, this reduction in applied stress allowed for differentiation between these two formulations for FP and identification of histidine as a stabilizing buffer salt.

Alternatively, decreasing the fill volume increases the V_{well}/V_{fill} ratio and applied stress. For the ADC, the increased stress applied while shaking at a reduced fill volume of 60 μL (V_{well}/V_{fill} 6) resulted in lower monomer recoveries relative to the original fill volume (100 μL) for all conditions other than ADC-His-P188 (Figure 6B). After shaking with a 60 μL fill volume, soluble aggregate content in ADC formulations containing PS20 and PS80 were greater by 4.5% [CI 3.4-5.6%] and 1.5% [CI 0.4-2.6%], respectively, compared to formulations containing P188. This increased stress resulted in clear delineation between the stabilizing effects of the three surfactants against interfacial stress in a microplate format, where the surfactants could be ranked from least to most stabilizing (PS20 < PS80 < P188). This ranking agreed with trends observed for monomer recovery and soluble aggregates after shaking the same formulations in vials. Further, this exemplifies that the lessons learned from fill volume studies of surfactant-free mAb1-His could be extrapolated to identify suitable conditions for evaluating surfactant-containing formulations. Whether this also applies to other parameters (e.g., sample concentration, plate material, shaking frequency and duration) will be an important question for future studies.

In the examples described above, the V_{well}/V_{fill} ratio was adjusted through changes in the fill volume. While this strategy allows different levels of interfacial stress to be applied within a single plate during a single shaking experiment, there may be instances where the fill volume cannot be changed. The V_{well}/V_{fill} ratio can also be adjusted through changes in the well volume V_{well} by selecting alternative plate formats. For example, deep-well plates or half-area plates to increase or reduce V_{well} , respectively. Overall, the V_{well}/V_{fill} ratio serves as an adjustable parameter that can be leveraged to tailor the applied interfacial stress.

Recommendations

In summary, we provide the following recommendations for the implementation of an orbital microplate shaking stress method. (1) Microplate shakers should be carefully tested for well position effects on protein aggregation and for possible heat dissipation. These effects should be checked periodically considering equipment durability issues. (2) Heat sealing is recommended for optimal seal integrity, thus avoiding well position effects by volume loss. If a heat sealer is not available, we recommend avoiding the outer microplate rows and verifying seal integrity visually after shaking.

(3) A shaking frequency (n) should be selected that is high enough to achieve comparable stress between samples by ensuring that all samples are in contact with the seal ($n > n_{max}$). However, it should not be so high as to promote well position effects that may be amplified near the shaker's operating maximum. When selecting n , differences in sample surface tension, viscosity, and fill volume should be considered as these properties may change n_{max} .

(4) As a starting point for method transfer, the parameter well volume to fill volume ratio V_{well}/V_{fill} should be used instead of the fill volume V_{fill} . To screen surfactant-free formulations, we recommend a V_{well}/V_{fill} of 3.6 for 24 h shaking at RT and 2400 rpm (a_c 95 m/s²). For surfactant screenings, the fill volume should be reduced to a V_{well}/V_{fill} of 6 to increase the applied interfacial stress.

CONCLUSION

This study provides an in-depth methodological account of miniaturized formulation screening by agitation-induced aggregation using orbital microplate shakers. Several sources of systemic bias, most notably from different shakers, can induce variable degrees of stress across the microplate, thereby increasing the risk for misleading formulation decisions. The findings revealed critical mechanistic factors of microplate-scale shaking, including a clear impact of the solution properties of formulations on liquid motion and pronounced aggregation upon liquid-seal contact. A thorough analysis of these biases and mechanistic features, as well as consequential recommendations for equipment, material and parameter selection have been provided. The good agreement of the presented microplate shaking method to results from vial shaking justifies its use for formulation screening in early development phases. The proposed method parameter V_{well}/V_{fill} will ease method transfer and comparability and may provide opportunities for further miniaturization.

ACKNOWLEDGEMENTS

The authors gratefully acknowledge Karl-Heinz Hergesell and his colleagues for sharing their expert knowledge on microplates and Michelle Zöller and her colleagues for their advice on surface tension measurements.

CONFLICTS OF INTEREST

The authors have no other relevant affiliations or financial involvement with any organization or entity with a financial interest in or financial conflict with the subject matter or materials discussed in the manuscript.

Journal Pre-proof

REFERENCES

1. Wang W. Instability, stabilization, and formulation of liquid protein pharmaceuticals. *Int J Pharm* 1999;185(2):129–188.
2. Wang W, Ohtake S. Science and art of protein formulation development. *Int J Pharm* 2019;568:118505.
3. Philippidis A. Genetic Engineering & Biotechnology News. Top 15 best-selling drugs launched in 2020. Available at: <https://www.genengnews.com/a-lists/top-15-best-selling-drugs-launched-in-2020>. Accessed January 18, 2021.
4. Moussa EM, Panchal JP, Moorthy BS, Blum JS, Joubert MK, Narhi LO, Topp EM. Immunogenicity of therapeutic protein aggregates. *J Pharm Sci* 2016;105(2):417–430.
5. Mahler H-C, Fischer S, Randolph TW, Carpenter JF. Protein aggregation and particle formation: Effects of formulation, interfaces, and drug product manufacturing operations. In: Wang W, Roberts CJ, eds. *Aggregation of Therapeutic Proteins, 1st ed.*, Hoboken N.J.: Wiley; 2010:301–331.
6. Li J, Krause ME, Chen X, Cheng Y, Dai W, Hill JJ, Huang M, Jordan S, LaCasse D, Narhi L, Shalaev E, Shieh IC, Thomas JC, Tu R, Zheng S, Zhu L. Interfacial stress in the development of biologics: Fundamental understanding, current practice, and future perspective. *AAPS J* 2019;21(3):44.
7. Shieh IC, Patel AR. Predicting the agitation-induced aggregation of monoclonal antibodies using surface tensiometry. *Mol Pharm* 2015;12(9):3184–3193.
8. Rudiuk S, Cohen-Tannoudji L, Huille S, Tribet C. Importance of the dynamics of adsorption and of a transient interfacial stress on the formation of aggregates of IgG antibodies. *Soft Matter* 2012;8(9):2651–2661.
9. Koepf E, Eisele S, Schroeder R, Brezesinski G, Friess W. Notorious but not understood: How liquid-air interfacial stress triggers protein aggregation. *Int J Pharm* 2018;537(1-2):202–212.
10. Koepf E, Schroeder R, Brezesinski G, Friess W. The film tells the story: Physical-chemical characteristics of IgG at the liquid-air interface. *Eur J Pharm Biopharm* 2017;119:396–407.
11. Dill S, Brees K, Stahly A, Cheng E, Carpenter J, Caplan L. Mechanical shock during shipping of medications: The roles of packaging and transportation vendors. *J Pharm Sci* 2020;109(1):670–676.
12. Siska C, Harber P, Kerwin BA. Shocking data on parcel shipments of protein solutions. *J Pharm Sci* 2020;109(1):690–695.
13. Bee JS, Schwartz DK, Trabelsi S, Freund E, Stevenson JL, Carpenter JF, Randolph TW. Production of particles of therapeutic proteins at the air–water interface during compression/dilation cycles. *Soft Matter* 2012;8(40):10329–10335.
14. Halley J, Chou YR, Cicchino C, Huang M, Sharma V, Tan NC, Thakkar S, Zhou LL, Al-Azzam W, Cornen S, Gauden M, Gu Z, Kar S, Lazar AC, Mehndiratta P, Smith J, Susic Z, Weisbach P, Stokes ESE. An industry perspective on forced degradation studies of biopharmaceuticals: Survey outcome and recommendations. *J Pharm Sci* 2020;109(1):6–21.

15. Goldberg DS, Lewus RA, Esfandiary R, Farkas DC, Mody N, Day KJ, Mallik P, Tracka MB, Sealey SK, Samra HS. Utility of high throughput screening techniques to predict stability of monoclonal antibody formulations during early stage development. *J Pharm Sci* 2017;106(8):1971–1977.
16. Niedziela-Majka A, Kan E, Weissburg P, Mehra U, Sellers S, Sakowicz R. High-throughput screening of formulations to optimize the thermal stability of a therapeutic monoclonal antibody. *J Biomol Screen* 2015;20(4):552–559.
17. He F, Hogan S, Latypov RF, Narhi LO, Razinkov VI. High throughput thermostability screening of monoclonal antibody formulations. *J Pharm Sci* 2010;99(4):1707–1720.
18. Ausar SF, Chan J, Hoque W, James O, Jayasundara K, Harper K. Application of extrinsic fluorescence spectroscopy for the high throughput formulation screening of aluminum-adsorbed vaccines. *J Pharm Sci* 2011;100(2):431–440.
19. Dasnoy S, Le Bras V, Pr eat V, Lemoine D. High-throughput assessment of antigen conformational stability by ultraviolet absorption spectroscopy and its application to excipient screening. *Biotechnol Bioeng* 2012;109(2):502–516.
20. He F, Woods CE, Becker GW, Narhi LO, Razinkov VI. High-throughput assessment of thermal and colloidal stability parameters for monoclonal antibody formulations. *J Pharm Sci* 2011;100(12):5126–5141.
21. Dasnoy S, Dezutter N, Lemoine D, Le Bras V, Pr eat V. High-throughput screening of excipients intended to prevent antigen aggregation at air-liquid interface. *Pharm Res* 2011;28(7):1591–1605.
22. Zhao H, Graf O, Milovic N, Luan X, Bluemel M, Smolny M, Forrer K. Formulation development of antibodies using robotic system and high-throughput laboratory (HTL). *J Pharm Sci* 2010;99(5):2279–2294.
23. Alekseychik L, Su C, Becker GW, Treuheit MJ, Razinkov VI. High-throughput screening and stability optimization of anti-streptavidin IgG1 and IgG2 formulations. *J Biomol Screen* 2014;19(9):1290–1301.
24. Casaz P, Brousseau A, Ozturk S. Development of a high-throughput formulation screening platform for monoclonal antibodies. *Bioprocess Int* 2015;13(8):48–59.
25. Floyd JA, Shaver JM, Gillespie AJ, Park U, Rogers RS, Nightlinger NS, Ogata Y, James JJ, Kerwin BA. Evaluation of crystal zenith microtiter plates for high-throughput formulation screening. *J Pharm Sci* 2020;109(1):532–542.
26. Eppler A, Weigandt M, Hanefeld A, Bunjes H. Relevant shaking stress conditions for antibody preformulation development. *Eur J Pharm Biopharm* 2010;74(2):139–147.
27. Vargas SK, Eskafi A, Carter E, Ciaccio N. A comparison of background membrane imaging versus flow technologies for subvisible particle analysis of biologics. *Int J Pharm* 2020;578:119072.
28. Buecheler JW, Winzer M, Weber C, Gieseler H. Oxidation-induced destabilization of model antibody-drug conjugates. *J Pharm Sci* 2019;108(3):1236–1245.

29. McGown EL, Hafeman DG. Multichannel pipettor performance verified by measuring pathlength of reagent dispensed into a microplate. *Anal Biochem* 1998;258(1):155–157.
30. Hermann R, Lehmann M, Büchs J. Characterization of gas-liquid mass transfer phenomena in microtiter plates. *Biotechnol Bioeng* 2003;81(2):178–186.
31. Bai G, Bee JS, Biddlecombe JG, Chen Q, Leach WT. Computational fluid dynamics (CFD) insights into agitation stress methods in biopharmaceutical development. *Int J Pharm* 2012;423(2):264–280.
32. McDonald GR, Hudson AL, Dunn SMJ, You H, Baker GB, Whittal RM, Martin JW, Jha A, Edmondson DE, Holt A. Bioactive contaminants leach from disposable laboratory plasticware. *Science* 2008;322(5903):917.
33. Olivieri A, Degenhardt OS, McDonald GR, Narang D, Paulsen IM, Kozuska JL, Holt A. On the disruption of biochemical and biological assays by chemicals leaching from disposable laboratory plasticware. *Can J Physiol Pharmacol* 2012;90(6):697–703.
34. Couston RG, Skoda MW, Uddin S, van der Walle CF. Adsorption behavior of a human monoclonal antibody at hydrophilic and hydrophobic surfaces. *mAbs* 2013;5(1):126–139.
35. Zidar M, Posnjak G, Muševič I, Ravnik M, Kuzman D. Surfaces affect screening reliability in formulation development of biologics. *Pharm Res* 2020;37(2):27.
36. Gerhardt A, McGraw NR, Schwartz DK, Bee JS, Carpenter JF, Randolph TW. Protein aggregation and particle formation in prefilled glass syringes. *J Pharm Sci* 2014;103(6):1601–1612.
37. Lin GL, Pathak JA, Kim DH, Carlson M, Riguero V, Kim YJ, Buff JS, Fuller GG. Interfacial dilatational deformation accelerates particle formation in monoclonal antibody solutions. *Soft Matter* 2016;12(14):3293–3302.
38. Fleischman ML, Chung J, Paul EP, Lewus RA. Shipping-induced aggregation in therapeutic antibodies: Utilization of a scale-down model to assess degradation in monoclonal antibodies. *J Pharm Sci* 2017;106(4):994–1000.
39. Wood CV, McEvoy S, Razinkov VI, Qi W, Furst EM, Roberts CJ. Kinetics and competing mechanisms of antibody aggregation via bulk- and surface-mediated pathways. *J Pharm Sci* 2020;109(4):1449–1459.
40. Treuheit MJ, Kosky AA, Brems DN. Inverse relationship of protein concentration and aggregation. *Pharm Res* 2002;19(4):511–516.
41. Kiese S, Pappengerger A, Friess W, Mahler H-C. Shaken, not stirred: Mechanical stress testing of an IgG1 antibody. *J Pharm Sci* 2008;97(10):4347–4366.
42. Büchs J, Lotter S, Milbradt C. Out-of-phase operating conditions, a hitherto unknown phenomenon in shaking bioreactors. *Biochem Eng J* 2001;7(2):135–141.
43. Gandhi AV, Randolph TW, Carpenter JF. Conjugation of emtansine onto trastuzumab promotes aggregation of the antibody-drug conjugate by reducing repulsive electrostatic interactions and increasing hydrophobic interactions. *J Pharm Sci* 2019;108(6):1973–1983.

44. Vargo KB, Stahl P, Hwang B, Hwang E, Giordano D, Randolph P, Celentano C, Hepler R, Amin K. Surfactant impact on interfacial protein aggregation and utilization of surface tension to predict surfactant requirements for biological formulations. *Mol Pharm* 2021;18(1):148–157.
45. Kopp MRG, Wolf Pérez A-M, Zucca MV, Capasso Palmiero U, Friedrichsen B, Lorenzen N, Arosio P. An accelerated surface-mediated stress assay of antibody instability for developability studies. *mAbs* 2020;12(1):1815995.

Journal Pre-proof

List of Figure Legends

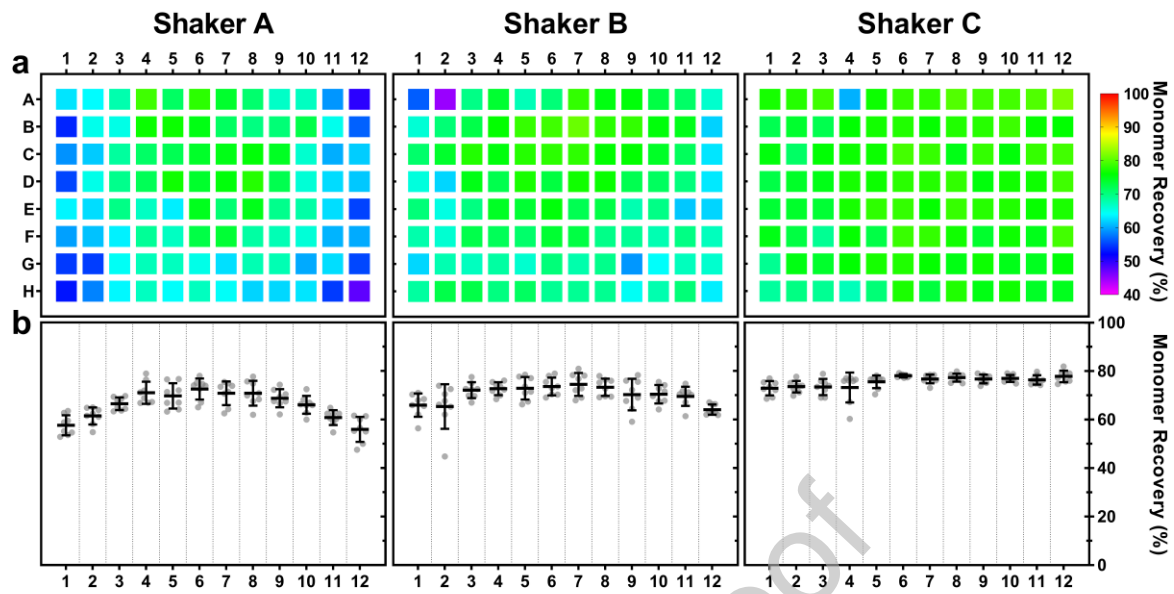


Figure 1. Dependence of mAb1-His monomer recovery on well position following 24 hours of shaking at $a_c \sim 100 \text{ m/s}^2$ for three different shakers. (a) Heat-map illustrating the position dependent variation in monomer recovery for plates shaken with each shaker. (b) Average monomer recovery (%) \pm standard deviation (black lines) for each microplate column. Individual values for each well within a column are displayed as grey circles.

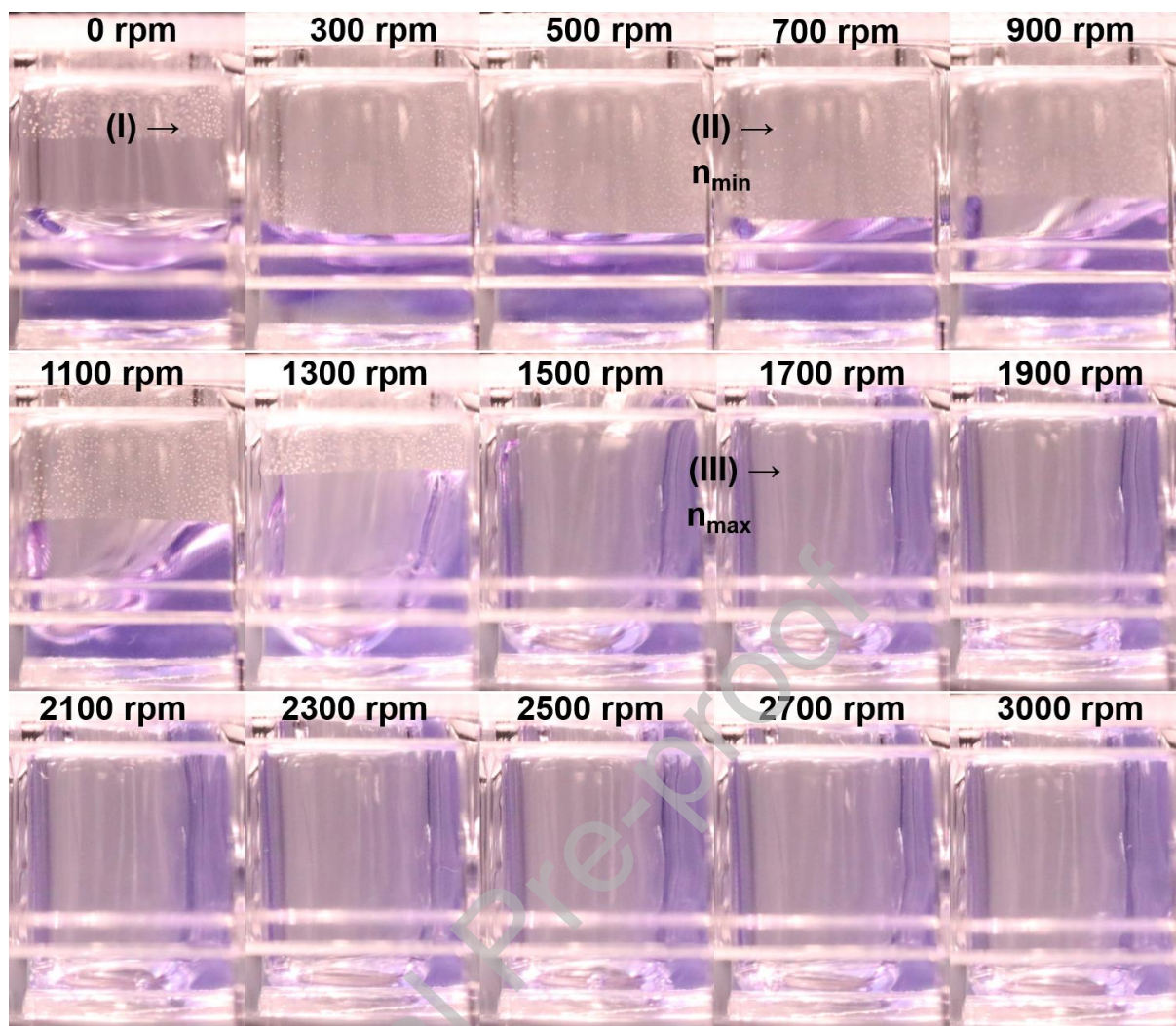


Figure 2. Exemplary images of microplate wells containing 100 µL of mAb1-His, stained with bromophenol blue at different shaking frequencies (well side view). Liquid motion is characterized by three stages (I-III).

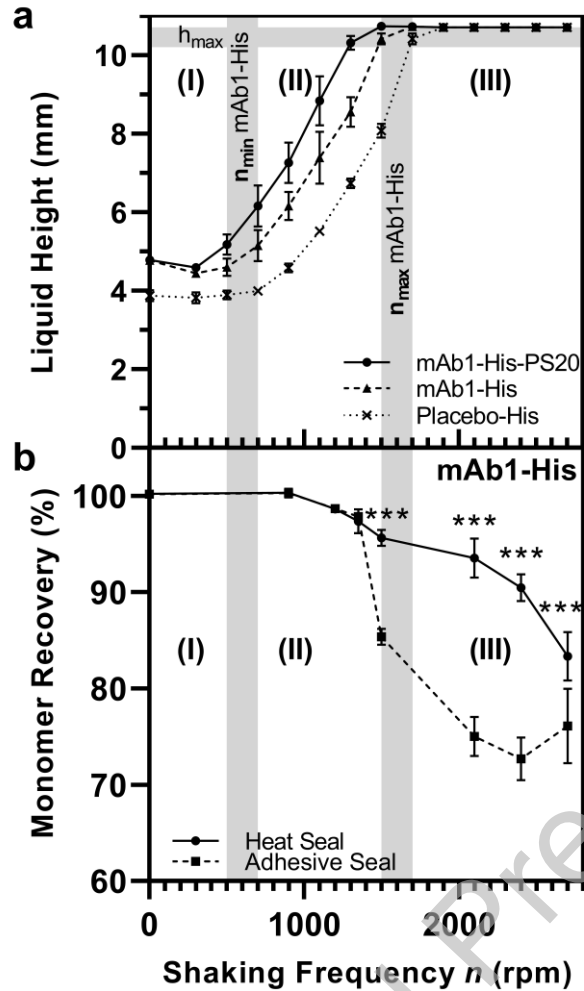


Figure 3. Correlation between liquid height during shaking and mAb1 monomer recovery. (a) Liquid height as a function of shaking frequency for placebo histidine formulation (crosses), mAb1-His (triangles) and mAb1-His-PS20 (circles). (b) Monomer recovery of mAb1-His after shaking for 24 hours at different shaking frequencies for plates sealed using either heat seals (circles) or adhesive seals (squares).

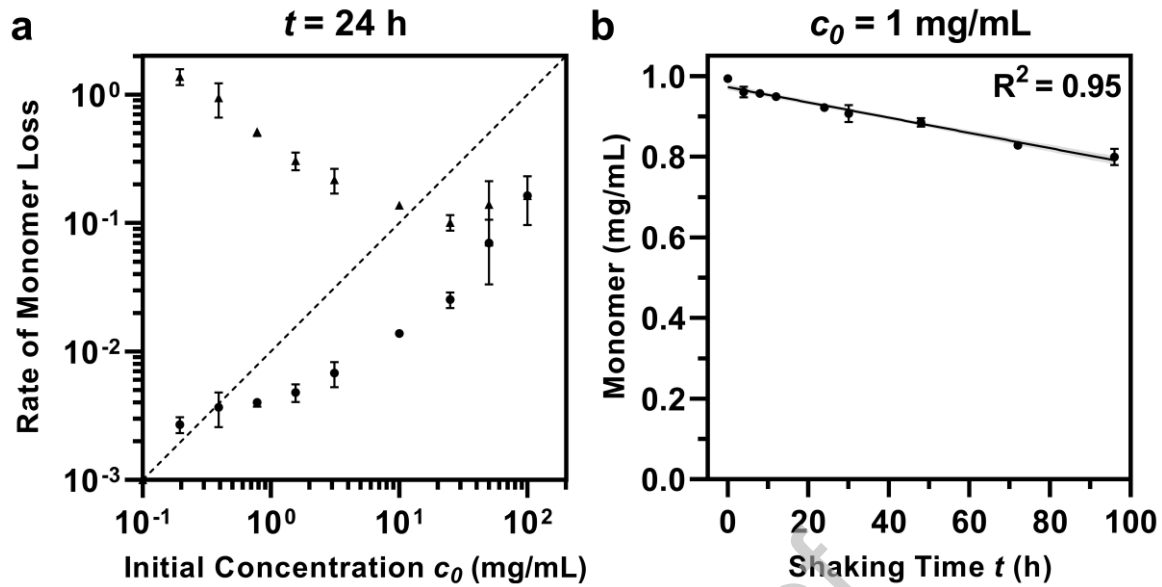


Figure 4. Effect of mAb1-His concentration and shaking time on mAb1-His monomer loss as measured by size exclusion chromatography. (a) Relative rates of monomer loss in $\% \cdot \text{h}^{-1}$ (triangles) and absolute rates in $\text{mg/mL} \cdot \text{h}^{-1}$ (circles) at different initial mAb1 concentrations c_0 after 24 hours of shaking. The slope of the dashed line indicates first order scaling of absolute monomer loss rates with protein concentration. (b) Monomer concentration as a function of shaking time over 96 hours of shaking at a c_0 of 1 mg/mL. Data were fitted by linear regression.

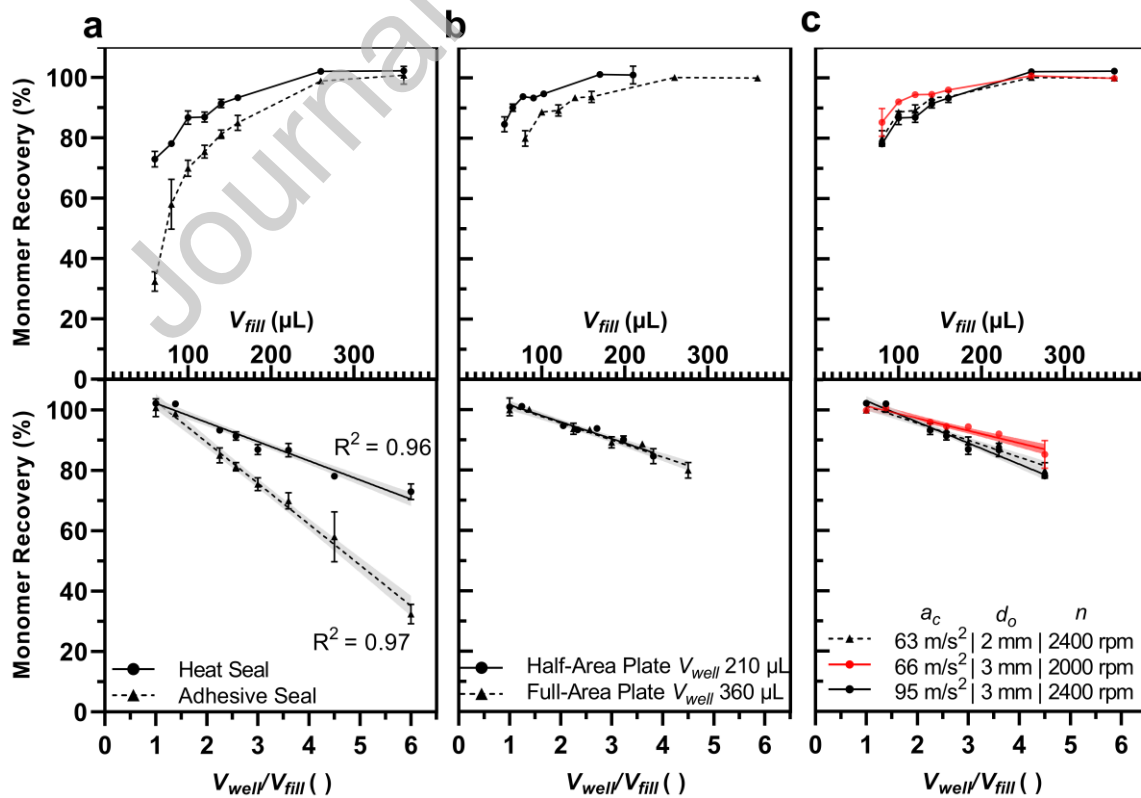


Figure 5. Monomer recovery of mAb1-His after shaking for 24 hours as a function of fill volume V_{fill} (top panel) and well volume to fill volume ratio V_{well}/V_{fill} (bottom panel) for (a) Shaker C at 2400 rpm and plates sealed with either heat seals (circles) or adhesive seals (triangles), (b) Shaker B at 2400 rpm with half-area plates (circles) or full-area plates (triangles), (c) Shaker C operated at either the same shaking frequency n (black circles) or similar centrifugal acceleration a_c (red circles) as to Shaker B (black triangles). Data plotted as a function of the V_{well}/V_{fill} ratio were fitted by linear regression and are depicted with a 95% CI (grey or red shades).

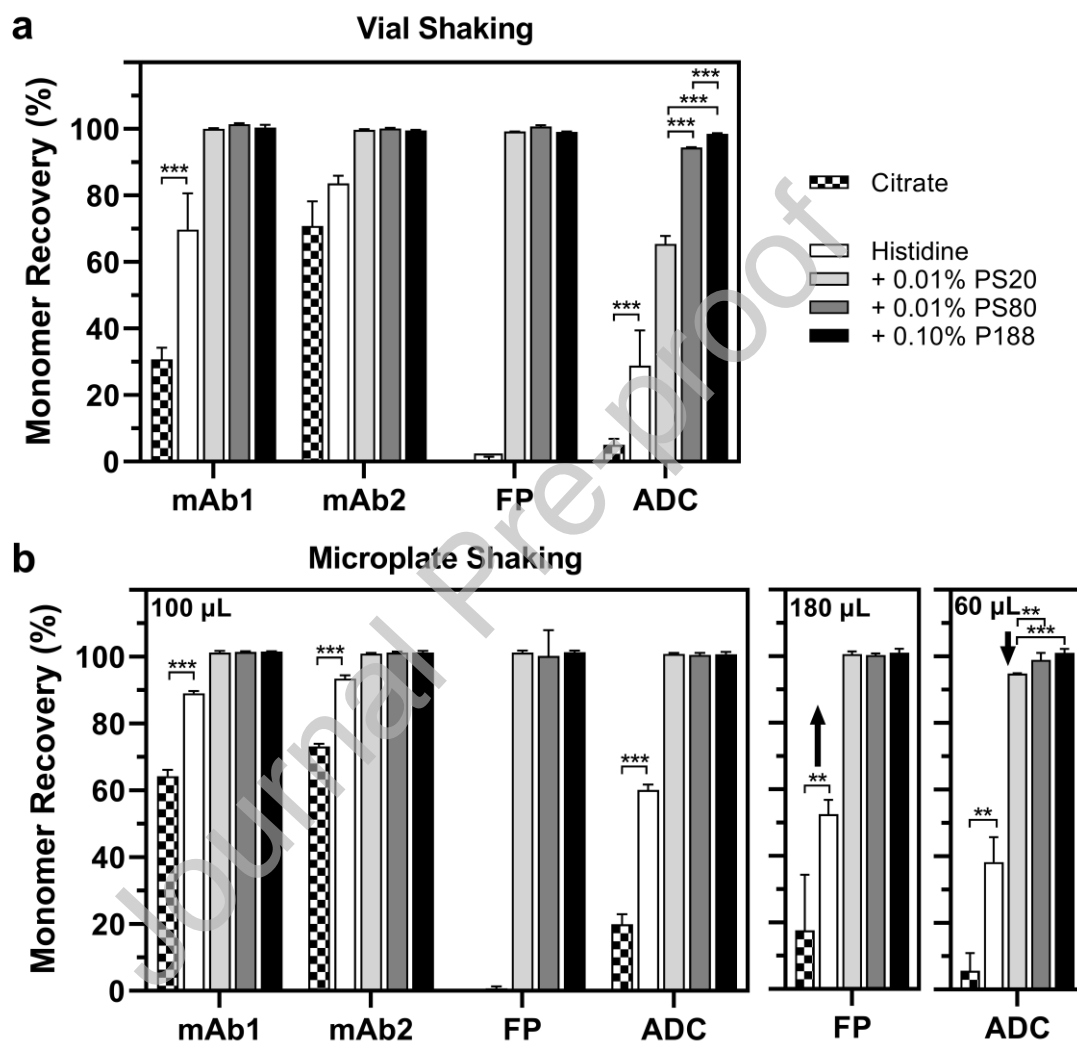


Figure 6. Comparison of mAb1, mAb2, FP and ADC stability after shaking in (a) vials or (b) microplates quantified by monomer recovery measured with SEC. Five formulations were evaluated for each molecule. Included formulations were composed of 10 mM citrate pH 5.5 (checkered bars) or 10 mM histidine pH 5.5 containing; no added excipients (white bars), 0.01% polysorbate 20 (light grey bars), 0.01% polysorbate 80 (dark grey bars) or 0.1% Poloxamer 188 (black bars). In addition, for FP and ADC the effect of three fill volumes (60, 100 and 180 µL) on monomer recovery after shaking in microplates were investigated.

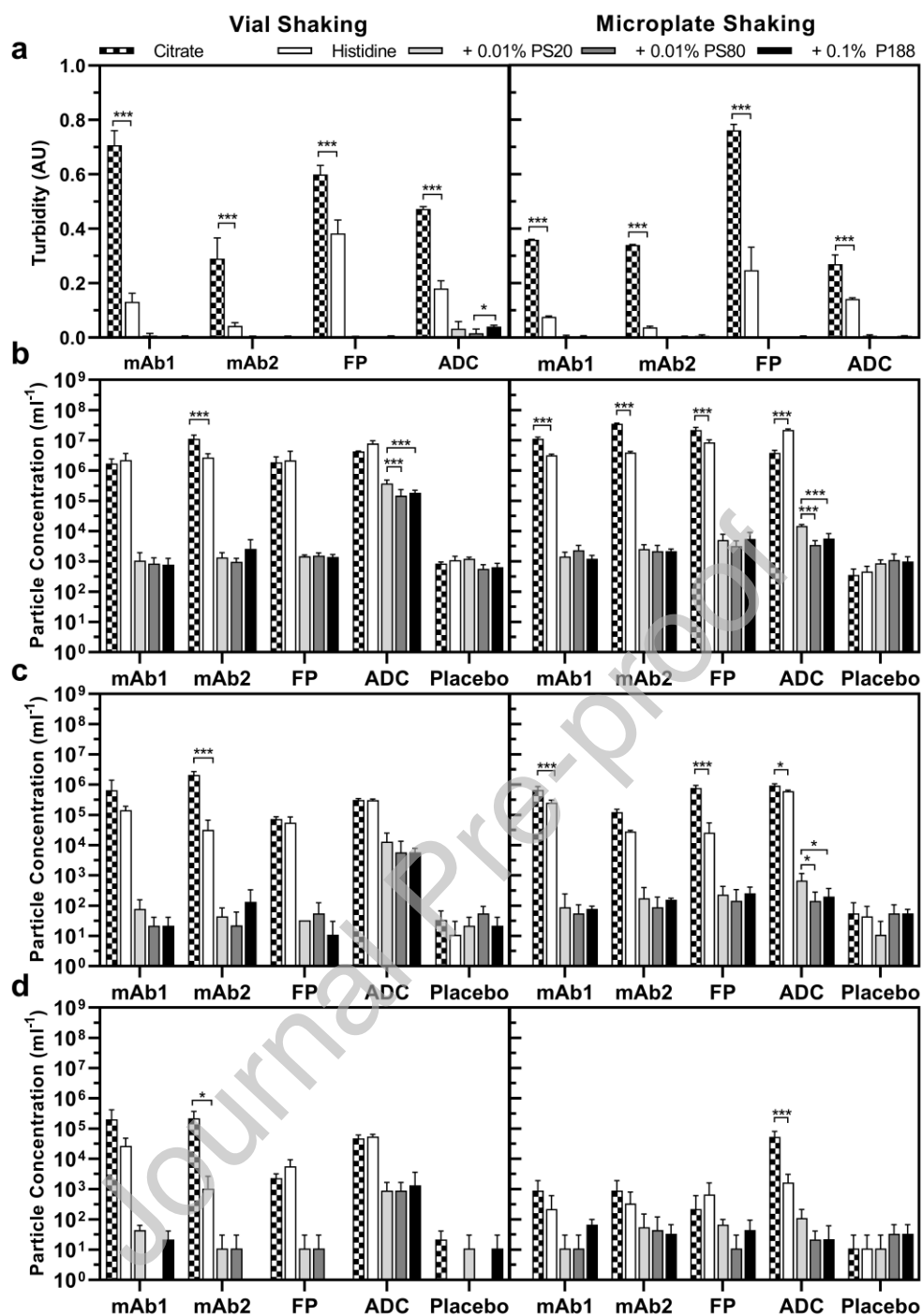


Figure 7. Comparison of mAb1, mAb2, FP and ADC stability after shaking in vials (left panels) or microplates (V_{fill} 100 μL) (right panels) quantified by (a) turbidity or the concentration (ml^{-1}) of particles (b) $\geq 2 \mu\text{m}$, (c) $\geq 10 \mu\text{m}$, and (d) $\geq 25 \mu\text{m}$ measured by backgrounded membrane imaging. Five formulations were evaluated for each molecule. Included formulations were composed of 10 mM citrate pH 5.5 (checkered bars) or 10 mM histidine pH 5.5 containing; no added excipients (white bars), 0.01% polysorbate 20 (light grey bars), 0.01% polysorbate 80 (dark grey bars) or 0.1% Poloxamer 188 (black bars).

Table 1. Properties of the Studied Shakers, Microplates and Seals.

Equipment	Notation	Vendor	Model/PN*	Properties		
				<i>Max. rpm</i>	<i>Shaking Orbit d_o Ø</i>	<i>Platform Stabilization</i>
Shaker	Shaker A	Grant Instruments	MPS-1	3200	3 mm	one central axis
	Shaker B	QInstruments	Bioshake iQ	3000	2 mm	multiple axes
	Shaker C	Eppendorf	MixMate	3000	3 mm	n/a**
				<i>Wells</i>	<i>Material</i>	<i>Well Dimension (mm)***</i>
Microplate	PA full-area	Corning	3635	96	Polyacrylate (PA)	10.7, 6.9, 6.4
	PA half-area	Corning	3679	96	Polyacrylate (PA)	11.5, 5.0, 4.5
	PP full-area	Corning	3364	96	Polypropylene (PP)	10.7, 6.9, 6.4
	PS full-area	Corning	3591	96	Polystyrene (PS)	10.7, 6.9, 6.4
				<i>Material</i>	<i>Application</i>	
Seal	Heat seal	4titude	4ti-0542	Copolymer, Polyester		Heat, 180 °C, 4 s
	Adhesive seal	BioChromato	REPS001	Polyolefin, Polyethylene terephthalate		Pressure, adhesive

* part number; the models were obtained in July 2020 ** n/a not available *** depth, top diameter, bottom diameter

Table 2. Summary of Experimental Designs for Microplate Shaking.

Study (Figure)	Shaker	<i>n</i> (rpm)	<i>t</i> (h)	<i>c</i> ₀ (mg/mL)	<i>V</i> _{fill} (µL)	<i>V</i> _{well} (µL)	Material	Seal Type**	<i>N</i>
<i>Equipment Suitability</i>									
Well Position Effects (1)	A / B / C	2500 / 3000 / 2500	24	1	100	360	PA	H	96
- impact of <i>n</i>	A	3000	5	1	100	360	PA	H	96
Seal Integrity	C	2500	24	n/a*	100	360	PA	H / A	96
<i>Parameters</i>									
Liquid Motion (2-3A)	C	0 – 3000	n/a*	1	100	360	PA	A	6
Shaking Frequency (3B)	C	0 – 2700	24	1	100	360	PA	H / A	12
Concentration (4A)	C	2400	24	0.2-100	100	360	PA	H	3
Time (4B)	C	2400	0-96	1	100	360	PA	H	4
Fill Volume (5A)	C	2400	24	1	60-360	360	PA	H / A	3
Well Size (5B)	B	2400	24	1	80-360 / 55-210	360 / 210	PA	H	3
Shaking Orbit (5C)	B / C / C	2400 / 2000 / 2400	24	1	80-360	360	PA	H	3
Plate Material	C	2400	24	1	100	360	PA / PP / PS	A	3

Comparability Vial vs.									
Microplate Shaking (6-7)	C	2400	24	1	100 (60 / 180)	360	PA	H	3
* n/a not applicable ** H: Heat seal, A: Adhesive seal									

Table 3. Intra- and Inter-plate Reproducibility of mAb1-His Monomer Recovery (%) using the Optimized Microplate Shaking Method.

Plate	Well 1	Well 2	Well 3
Plate 1	89.8	88.4	89.0
Plate 2	91.6	89.2	91.2
Plate 3	91.6	92.1	91.4